COBEM 2023 27TH INTERNATIONAL CONGRESS OF MECHANICAL ENGENEERING

ABCM Brazilian Society of Mechanical Sciences and Engineering
27th ABCM International Congress of Mechanical Engineering
December 04-08, 2023, Florianópolis-SC, Brazil

COB-2023-0267
Hands-on Activity with an Unconventional Harmonic Oscillator

Vinícius Lamas von Sohsten
Rubens Gonçalves Salsa Junior
Fabio Dalmazzo Sanches
Universidade Federal do Rio Grande do Norte, Lagoa Nova – Natal/RN - Brazil
vinicius.von.059@ufrn.edu.br, rubens.salsa@ufrn.br, fabio.dalmazzo@ufrn.br

Abstract. *Dynamics and vibrations are core branches of mechanical engineering that play a significant role in modeling and analysis of mechanical systems. These courses provide students with a strong foundation to pursue their studies and professional careers in various fields such as design, biomechanics, mechanics of solids, mechanisms, and control. However, the abstract nature of these subjects may be problematic and, not surprisingly, some of the biggest difficulties reported by students include difficult tom understand and visualize the problems, lack of physical and mathematical tools to represent phenomena and interpret results. To overcome these challenges, educators are moving away from the theoretical approach to a balanced combination of concrete experience and analysis. To fill in the gaps that exist due to poor laboratory infrastructure in some universities, there is a tendency to create practical activities using everyday objects, just as in teaching geometry there is a preference for simplistic constructions using compass and ruler. In this regard, this paper describes a practical classroom activity for dynamics/vibrations courses that involves analyzing the rocking motion of a semicylinder. The students are required to derive the nonlinear equation of motion involving the angular coordinate and linearize it under the assumption of small motions. This is followed by computation of the natural frequency of oscillation, which is compared to that of the real semicylinder when released from rest. This hands-on activity allows students to validate theoretical results by testing models they have built themselves. It also helps connect mathematical concepts with physical reality, making it easier for students to understand and visualize the problems. Practical activities such as the one described in this paper help students to actively engage with the coursework, develop practical skills, and bridge the gap between theory and practice. Additionally, it provides students with a platform to test new ideas and concepts, highlighting the importance of active learning through experimentation.*

Keywords: *Active learning, dynamics, Vibrations, Experiments, Harmonic Motion*

1. INTRODUCTION

Mechanical engineers possess a fundamental interest in comprehending how systems, which consist of various components working together, respond to different stimuli. Rather than conducting physical tests on every possible scenario, engineers employ mathematical representations to describe the behavior of these systems, a process known as modeling. The core disciplines within mechanical engineering undergraduate curricula primarily focus on modeling and analysis, which, in turn, are inherently abstract. Not surprisingly, students often encounter significant challenges in these disciplines, particularly in visualizing and understanding complex problems, lacking the necessary physical and mathematical tools to represent phenomena, and struggling to translate equations into tangible real-world situations. Consequently, they often show diminished motivation to engage fully with these fundamental engineering disciplines.

To overcome this issue, it may be necessary to embrace practical activities involving the construction of simple physical systems. The idea is that, just as in geometry teaching there is a preference for simplistic constructions using a compass and ruler, in engineering education there are advantages to using practical activities with engineering systems created using everyday items available to students, prioritizing simplicity (Casey, 1988). This approach is useful to address gaps that cannot be filled through laboratory activities, specially when many lab equipaments became inoperable due to prolonged unused time during the the COVID-19 pandemic lockdown.

These activities aim to translate abstract models into real-life situations, thereby facilitating the assimilation of basic concepts (Jensen *et al.*, 2003). This approach aligns with the contemporary belief that engineering education is shifting from a purely theoretical emphasis to a balance between hands-on experiences and analysis (Azhikannickal, 2019; Pusca *et al.*, 2017). Practical activities also hold significance within the problem-based learning approach, as they address real challenges and foster teamwork and problem-solving skills (Kolmos and De Graaff, 2003). This active learning approach prepares students for professional engineering practice, where practical skills and the ability to apply theoretical knowledge in real situations are essential (Feisel and Rosa, 2003).

Motivated by these observations, the objective of this work is to report on an hands-on activity for teaching and integrating the disciplines of dynamics and vibrations. This activity is concerned with the rocking motion of a semicylinder. Firstly, a simplified model involving a rigid body in planar motion is constructed. The equation of motions is derived using fundamental Newton-Euler dynamics and the theoretical frequency for small vibrations is obtained using the various tools from calculus. These results are compared with the oscillatory motion of a real-life semicylider constructed of wood. In addition, the angle of release is varied to showcase nonlinear effects. This practical activity provides students with a more comprehensive understanding of the principles of dynamics and vibrations, preparing them to face the real challenges encountered in the professional practice of engineering. This paper is organized as follows. The mathematical model of the rocking semicylinder is derived in Sec. 2. The experimental set up is depicted in Sec. 3. A summary is presented in Sec. 5.

2. MATHEMATICAL MODEL

In this section, the mathematical model is developed to derive the frequency for small oscillations. A list of variables used in the paper are shown in Table 1.

Table 1. List of variables used in the paper.

Variable	Description	Unit
θ	Semicylinder rotation angle	rad
R	Semicylinder Radius	m
m	Semicylinder mass	kg
I_{zz}	Semicylinder momentum of inertia	kg.m²
O	Origin of Newtonian space	—
C	Semicylinder center of mass	—
P	Instantaneous point of contact between the semicylinder and the floor	—
A	Geometric center of the flat face of the semycilinder	—
g	Gravity	m²/s
x	Horizontal distance from O to A	m
$\mathbf{x}_P$	Position vector of point P	m
$\bar{\mathbf{x}}$	Position vector of point C	m
$\mathbf{x}_A$	Position vector of point A	m
h	Distance from point A to point C	m
$\mathbf{N}$	Normal force	N
$\mathbf{F}_f$	Friction force	N
$\mathbf{H}$	Angular momentum of the semicylinder	kg.m²/s
$\mathbf{M}$	Resultant moment about the center of mass C	N.m
ω_n	Natural frequency of oscillation	rad/s
t	Time	s
T	Period of oscillation	s

2.1 Kinematic Analysis

Consider the rigid circular semicylinder shown in Fig. 1. Let $\{\mathbf{i}, \mathbf{j}, \mathbf{k} = \mathbf{i} \times \mathbf{j}\}$ be a fixed orthonormal basis in a Newtonian frame of reference O and $\{\mathbf{e}_1, \mathbf{e}_2, \mathbf{e}_3\}$ a right-handed orthonormal basis

$$\begin{aligned} \mathbf{e}_1 &= \cos\theta\,\mathbf{i} + \sin\theta\,\mathbf{j}, \\ \mathbf{e}_2 &= -\sin\theta\,\mathbf{i} + \cos\theta\,\mathbf{j}, \\ \mathbf{e}_3 &= \mathbf{k}, \end{aligned} \tag{1}$$

that is fixed on the body and is called corotational basis. The rotation angle θ of the corotational basis represents the tilt of the semicylinder relative to the horizontal plane.

In addition, a coordinate x is used to represent the position of point A according to

$$\mathbf{x}_A = x\mathbf{i}. \tag{2}$$

This means the position of the center of mass C may be represented as

$$\bar{\mathbf{x}} = \mathbf{x}_A - h\mathbf{e}_2, \tag{3}$$

where

$$h = \frac{4R}{3\pi}. \tag{4}$$

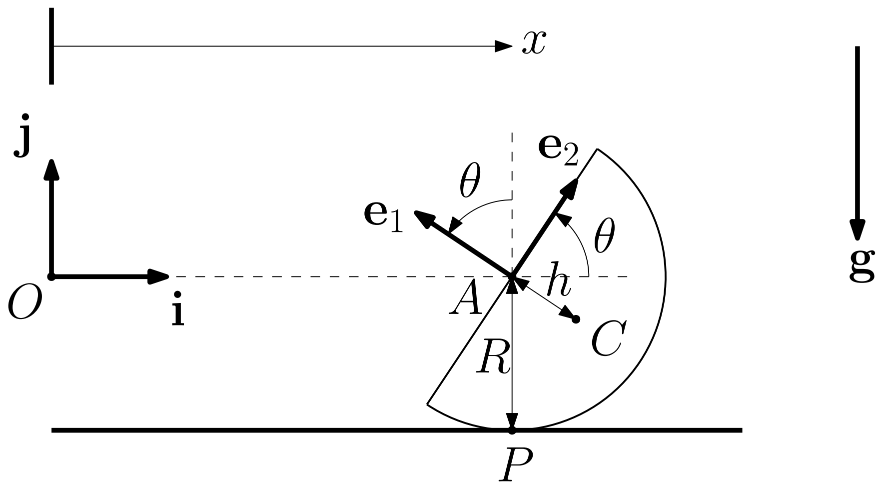

Figure 1. A rigid semicylinder with radius R, mass m and moment of inertia I_{zz} about the axis $\mathbf{e}_3 = \mathbf{k}$ passing through its center of mass C. The gravitational force acts in the $-\mathbf{j}$ direction.

The semicylinder moves under the rolling regime, so the instantaneous point of contact P has zero velocity and the motion satisfies the holonomic constraint (Meriam *et al.*, 2015)

$$\dot{x} + R\dot{\theta} = 0 \Longrightarrow \ddot{x} + R\ddot{\theta} = 0. \tag{5}$$

2.2 Obtaining the Equation of Motion

The FBD of the system is shown in Fig. 2. The normal force $\mathbf{N}$ and friction force $\mathbf{F}_f$ act on the instantaneous point of contact P to maintain the rolling condition. In addition, the weight $-mg\mathbf{j}$ acts on the center of mass m.

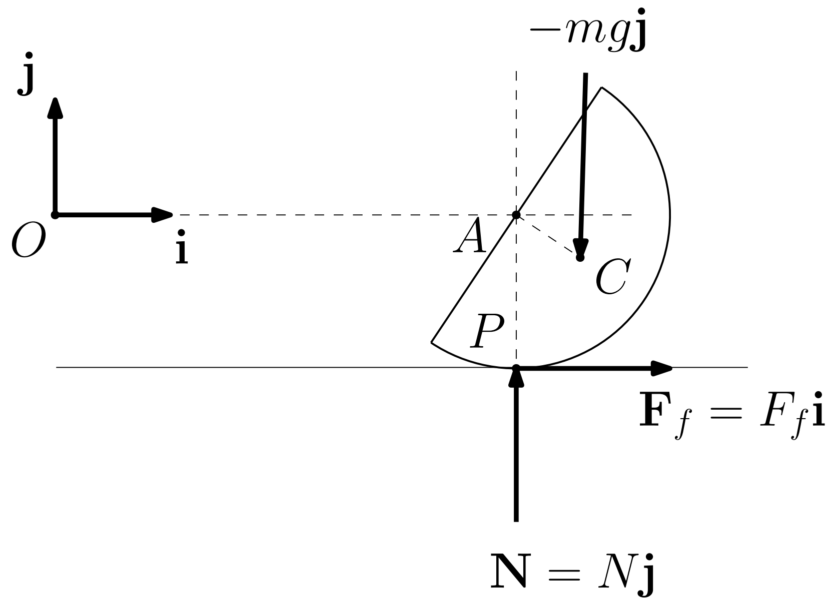

Figure 2. Free body diagram of the semicylinder.

Application of the balance of linear momentum together with the rolling restriction (5) yields

$$\mathbf{F} = m\bar{\mathbf{a}} \Longrightarrow \mathbf{F}_f + \mathbf{N} = m\left[\ddot{\theta}(h\mathbf{e}_1 - R\mathbf{i}) + R\dot{\theta}^2\mathbf{e}_2 + g\mathbf{j}\right]. \tag{6}$$

Similarly, the balance of angular momentum gives

$$\dot{\mathbf{H}} \cdot \mathbf{k} = \mathbf{M} \cdot \mathbf{k} = \dot{\mathbf{H}} \cdot \mathbf{k} \Longrightarrow I_{zz}\ddot{\theta} = (\mathbf{x}_P - \bar{\mathbf{x}}) \times (\mathbf{F}_f + \mathbf{N}) \cdot \mathbf{k}. \tag{7}$$

Since $\mathbf{x}_P - \bar{\mathbf{x}} = h\mathbf{e}_2 - R\mathbf{i}$ and using the properties of vector triple products, this equation simplifies to

$$I_{zz}\ddot{\theta} = (h\mathbf{e}_2 - R\mathbf{i}) \cdot (\mathbf{F}_f + \mathbf{N}). \tag{8}$$

Substituting Eq. (6) into (8), one arrives at the equation of motion

$$[I_{zz} + m(R^2 + h^2) - 2mRh\cos(\theta)]\ddot{\theta} + mRh\dot{\theta}^2\sin(\theta) + mgh\sin(\theta) = 0. \tag{9}$$

This is a second-order nonlinear ordinary differential equation that could be integrated for $\theta(t)$ given the initial conditions $\theta(t = 0)$ and $\dot{\theta}(t = 0)$.

2.3 Natural Frequency of Small Vibrations

Exact solutions for nonlinear equations of motion are possible to be obtained in closed form expressions only for the relatively few nonlinear systems whose equations of motion have specific forms. Consequently, engineers often rely on approximate and graphical solutions for these cases, frequently resorting to numerical methods. The equation of motion (9) may be approximated for small oscillations around $\theta = 0$. Taylor expanding this equation and retaining only first-order terms, the following linearized differential equation of motions is obtained (Rao, 2011)

$$\ddot{\theta} + \omega_n^2\theta = 0, \tag{10}$$

where

$$\omega_n = \sqrt{\frac{mgh}{I_{zz} + m(R - h)^2}}. \tag{11}$$

If the semicylinder is given a small initial angular displacement θ_0 and released from rest, i.e., $\dot{\theta}(t = 0) = 0$, then Eq. (10) can be solved to yield

$$\theta(t) = \theta_0\cos(\omega_n t). \tag{12}$$

Therefore, the semicylinder oscillates harmonically with natural frequency of oscillation ω_n. The period of oscillatory motion is

$$T = \frac{2\pi}{\omega_n}. \tag{13}$$

The linearization of the equation of motion was performed to simplify the mathematical analysis of the system. For small oscillations around the equilibrium position, linearization allows approximating the nonlinear behavior of the system with a simpler linear model, facilitating the solution of the differential equation and obtaining an analytical solution.

3. EXPERIMENTAL SETUP

The investigation of the oscillating semicylinder involved the following carefully planned experimental setup:

1. Construction of the Semicylinder Body: a semicylinder body was meticulously crafted using wood, with a chosen radius R as specified in Tab. 2. The selection of the material was based on its suitability for the experiment and ease of construction.

2. Assembly of the Experimental Setup: the setup was meticulously put together to provide support for the semicylinder, allowing it to oscillate freely. This setup included a stable base, an accurately calibrated angled scale divided into 10° intervals, and a tripod to stabilize the smartphone used for recording.

3. Measurement Procedure: to measure the angular displacement of the semicylinder during oscillation, an angled scale was positioned behind it as a visual reference, as shown in Fig. 5. By aligning the semicylinder with the divisions on the scale, we were able to precisely determine its angular displacement.

4. Initial Displacement: the semicylinder was manually displaced from its equilibrium position to a small initial angle as depicted in Fig. 3. Great care was taken to ensure consistent and reproducible displacement for each trial, eliminating any potential sources of error.

5. Release and Data Recording: once the semicylinder was positioned at the desired initial angle, it was released from rest, allowing it to oscillate freely. A smartphone camera, recording at a high frame rate of 240 frames per second, captured the entire motion of the body during its oscillations.

6. Data Analysis: the recorded video data was subjected to thorough analysis to determine the period of oscillation. This involved using advanced image analysis techniques to track the angular position of the body over the first three oscillations.

7. Repetition for Accuracy: to ensure reliability and minimize errors, the experimental procedure was repeated multiple times. This repetition allowed for the calculation of an average period of oscillation, accounting for any variations or inconsistencies in the experimental setup or initial conditions.

By meticulously following this experimental procedure, we were able to accurately determine the period of oscillation for the semicylinder. This data can be compared with theoretical predictions to validate the analytical model and gain valuable insights into the dynamic behavior of the system.

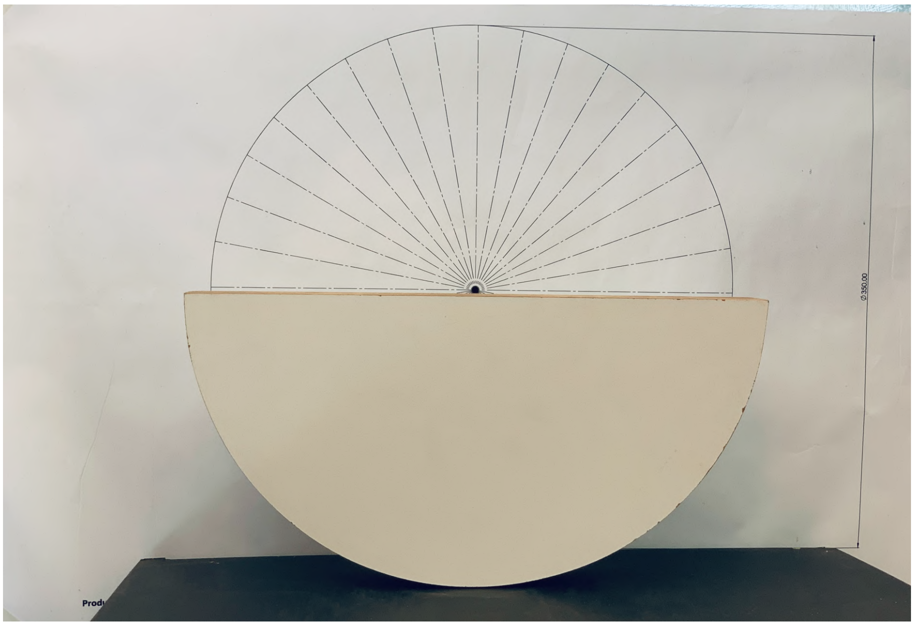

Figure 3. Wood Semicylinder standing on a horizontal bench. The angle scale is placed behind it.

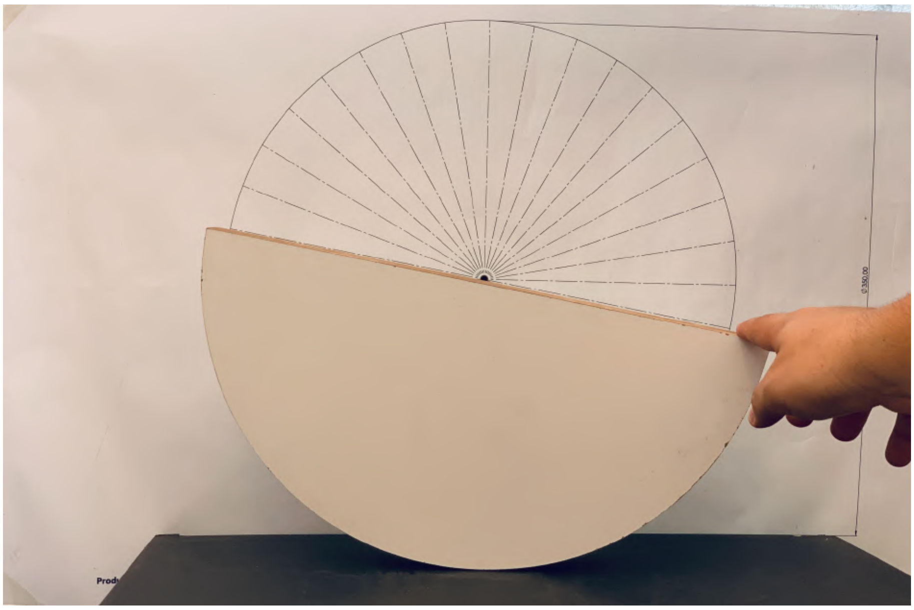

Figure 4. Semicylinder with initial angular displacement $\theta_0 = 10°$ released from rest.

4. RESULTS

The main results are expounded in this section.

4.1 Theoretical Period of Small Oscillations

The period of oscillation T can be expressed in terms of the radius R by substituting the expression for the moment of inertia

$$I_{zz} = \left(\frac{1}{2} - \frac{16}{9\pi^2}\right) mR^2 \tag{14}$$

into Eq. 13. The expression for T is then given by:

$$T = 2\pi\sqrt{\frac{R}{4g}\left(\frac{9\pi}{2} - 8\right)} \tag{15}$$

It is noteworthy that the mass of the body does not influence the period of oscillation, only the radius does. As the radius increases, the period of oscillation also increases. To illustrate this relationship, a graph of T as a function of R can be plotted, as shown in Figure 4.

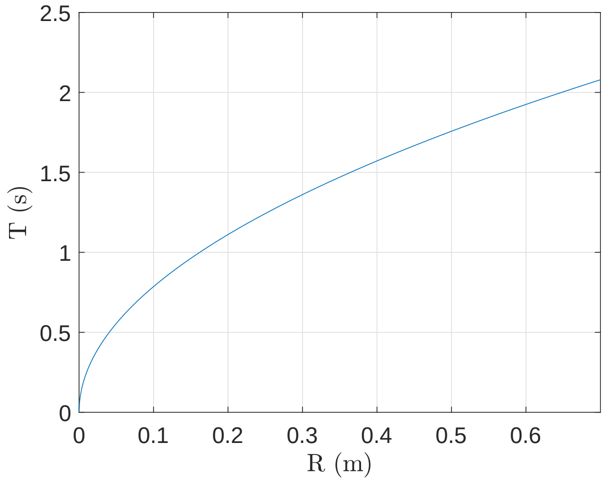

Figure 5. Period of oscillation as a function of the semicylinder radius.

Considering that the mass does not affect the period, the choice of material for constructing the semicylinder was based on availability and cost-effectiveness, prioritizing practicality for the experimental setup. In order to achieve a system with a period of oscillation of approximately one second, a radius of $R = 0.175$ m was selected. This choice resulted in a semicylinder of reasonable size for conducting the experiment, allowing for convenient observation and measurement of the period. Subsequently, with the chosen radius, it is possible to calculate the theoretical natural frequency and, consequently, the theoretical period of oscillation (15), as shown in Table 2.

Table 2. Semicylinder parameters.

Properties	Values
R, m	0.175
g, m²/s	9.81
h, m	0.07427
I_{zz}, kg.m²	0.00980
T, s	1.0395

4.2 Experimental Verification

An experimental investigation was conducted to determine the accuracy of the theoretical results. The semicylinder was initially released from rest, with angular displacements of $\theta_0 = 5°, 10°, 15°$, and $20°$. The period was measured for the first three complete oscillations corresponding to each initial angular displacement. The recorded data can be found in Table 3.

To assess the agreement between the experimental and theoretical findings, the average time required to complete the first three oscillations was calculated. The analytical results from Table 2 and the experimental measurements are compared in Tab. 4. It is important to note that the period predicted by small oscillations assumption is independent of initial

Table 3. Time to undergo a complete oscillation.

	Time, s			
θ_0	5°	10°	15°	20°
1st oscillation	0.9893	1.0583	1.0490	1.0630
2nd oscillation	0.9750	1.0637	1.0513	1.0733
3rd oscillation	0.9693	1.0327	1.0727	1.0677

conditions, therefore it offers good agreement with measured data only for small amplitudes. In fact, the measurements indicate that the period increases as the release angle is enlarged, indicating the influence of nonlinear effects for larger displacements. Additionally, the slight deviation between the analytical and experimental results for $\theta_0 = 5°$ and $10°$ can be attributed to measurement errors arising from challenges in accurately identifying the precise oscillation cycle and minor geometric imperfections in the semicylinder's perimeter.

Table 4. Comparison of analytical and experimental measurements for the natural period of oscillation.

	T, s		
$\boldsymbol{\theta_0}$	**Period for Small Motions**	**Measure Period**	**Period from Nonlinear ODE**
5°	1.0395	0.9779	1.0432
10°	1.0395	1.0516	1.0482
15°	1.0395	1.0577	1.0514
20°	1.0395	1.0680	1.0640

In the case of larger initial displacements, nonlinear effects become dominant, rendering the approximate linear model inadequate due to its amplitude-independent predicted period. To estimate the theoretical period of oscillation in such cases, the nonlinear equation of motion was numerically integrated, and the response $\theta(t)$ was analyzed. The numerical integration of the nonlinear ODE (9) was performed using MATLAB's ode45 solver, and a representative response $\theta(t)$ is depicted in Fig. 6. It can be observed that for $\theta_0 = 15°$ and $20°$, the experimental values align well with the period estimated from a plot like the one presented in Fig. 6. Furthermore, the increase in period between successive angular displacements remains consistent, further confirming the prevalence of nonlinear effects for larger initial displacements.

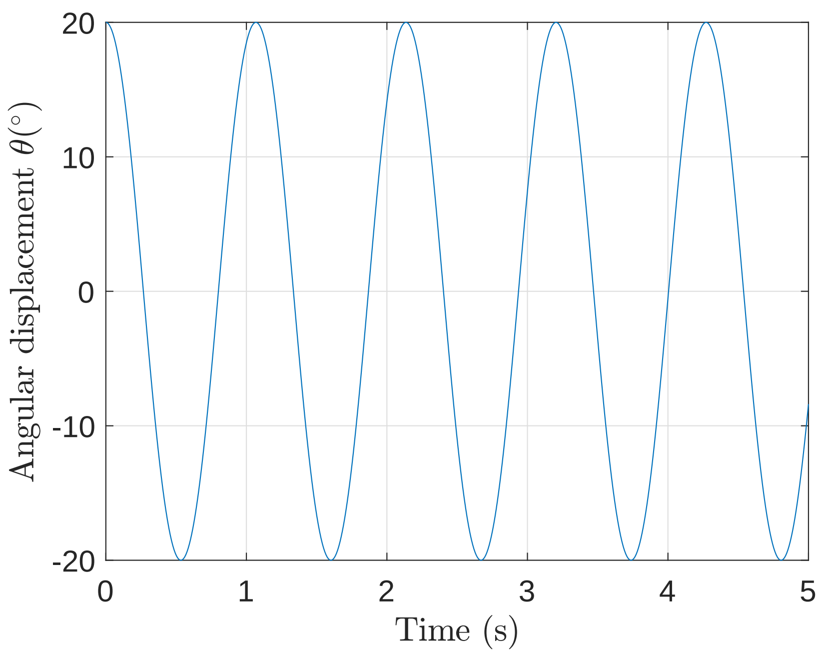

Figure 6. Angular displacement of the cylinder for large amplitudes. This curve was produced by numerically integrating Eq. (9) with the initial conditions $\theta_0 = 20°$ and $\dot{\theta}_0 = 0$.

5. SUMMARY

This study introduces a practical classroom activity designed for dynamics/vibrations courses, specifically focusing on the analysis of the rocking motion of a semicylinder. The activity involved various steps, including deriving the nonlinear equation of motion, linearizing it based on small motion assumptions, calculating the natural frequency of oscillation, and numerically integrating the equation of motion. By comparing the calculated period of oscillation with the observed of an physical semicylinder, students are able to validate the theoretical models they developed. This activity effectively combined hands-on experiences with theoretical analysis and numerical computing, enabling students to establish connections between mathematical concepts and real-world phenomena. Such approach not only enriches the learning experience but also fosters inclination to explore new ideas and concepts, emphasizing the significance of active learning through experimentation.

6. ACKNOWLEDGEMENTS

The authors would like to acknowledge the financial support from UFRN through an Educational Project Grant for the 2023 academic year.

This study was financed in part by the Coordenação de Aperfeiçoamento de Pessoal de Nível Superior - Brasil (CAPES) - Finance Code 001

7. REFERENCES

Azhikannickal, E., 2019. "Sports, smartphones, and simulation as an engaging method to teach projectile motion incorporating air resistance". *The Physics Teacher*, Vol. 57, p. 57.

Casey, J., 1988. "The bobbing buoy". *The Physics Teacher*, Vol. 26, p. 33.

Feisel, L.D. and Rosa, A.J., 2003. "The role of the undergraduate laboratory in undergraduate engineering education". *Journal of Engineering Education*, Vol. 94, pp. 121–130.

Jensen, D., Wood, J. and Wood, K., 2003. "Hands-on activities, interactive multimedia and improved team dynamics for enhancing mechanical engineering curricula". *International Journal of Engineering Education*, Vol. 9, p. 6.

Kolmos, A. and De Graaff, E., 2003. "The characteristics of problem-based learning". *International Journal of Engineering Education*, Vol. 19, pp. 657–662.

Meriam, J.L., Kraige, L.G. and Bolton, J.N., 2015. *Engineering Mechanics: Dynamics*. Wiley, Hoboken, New Jersey, 8th edition.

Pusca, D., Bowers, R.J. and Northwood, D.O., 2017. "Hands-on experiences in engineering classes: The need, the implementation and the results". *World Transactions on Engineering and Technology Education*, Vol. 15, p. 15.

Rao, S.S., 2011. *Mechanical Vibrations*. Prentice Hall, Upper Saddle River, New Jersey, 5th edition.

8. RESPONSIBILITY NOTICE

The authors are solely responsible for the printed material included in this paper.